Bonding in amorphous carbon-nitrogen alloys: A first principles study

Ariel A. Valladares*
Instituto de Investigaciones en Materiales, UNAM, Apartado Postal 70-360, México D.F., 04510, Mexico

Fernando Álvarez-Ramírez
Programa de Ingeniería Molecular, IMP, Eje Central Lázaro Cárdenas 152, México D.F., 07730, Mexico
(Received 8 August 2005; revised manuscript received 16 December 2005; published 25 January 2006)

An analysis of the bonding structure of nine different amorphous carbon-nitrogen alloys, a-$C_{1-x}N_x$, of concentrations $0 \leqslant x \leqslant 0.45$, is performed on *ab initio* generated atomic random networks. 216-atom periodically-continued cubic diamondlike supercells containing carbons and randomly substituted nitrogens were amorphized by "heating" them to a value *below* the melting temperature, using a Harris-functional based *ab initio* molecular dynamics code. After quenching, annealing, and optimizing, amorphous atomic structures were obtained where the nature of the bonding was studied using a cutoff determined by the first minimum of the corresponding partial radial distribution function. We find that, for *low concentrations*, tetravalent nitrogen is predominant, in agreement with experiment. For concentrations near 30% nitrogen molecules appear signaling the onset of the doping limit observed by experimentalists.

DOI: 10.1103/PhysRevB.73.024206 PACS number(s): 71.23.Cq, 71.15.Pd, 71.55.Jv

I. PREAMBLE AND ANTECEDENTS

It is well known that carbon is a versatile element due to the variety of hybridization states that it assumes and this leads to a multiplicity of bond arrangements fostering the formation of compounds with varied structures.[1,2] This versatility is reflected in its amorphous phase which, depending on its density, may have atomic arrangements that go from polymericlike to diamondlike, including graphitic structures; that is, the study of amorphous carbon is a density dependent issue. Nitrogen also manifests several possible bonding arrangements, and when it is incorporated into amorphous carbon the variety of structures that can be formed is evidently much greater,[3] exhibiting up to 9 different competing forms. These structures are also density dependent.[4] It is then clear that the description of the bonding nature of the amorphous carbon-nitrogen system can be highly complex, and the unambiguous identification of the bonding types may be difficult.

The experimental density of the CN system depends drastically on the specific process used to generate the material, and not just on the nitrogen concentration.[5] At this stage the dispersion in the experimental correlation (density) vs (concentration) is large and trying to find a systematic behavior becomes difficult.

There is a need to understand amorphous CN since it is a potentially useful material in diverse applications. With nitrogen incorporation, amorphous carbon changes its electrical and optical properties[6,7] and chemical reactivity.[8] It is also important to study the effect that the incorporation of nitrogen into an amorphous carbon matrix has on the bonding structure. This knowledge would allow one to tailor these structures to display specific properties. It is experimentally known that resistivities and optical band gaps decrease, compared to the pure *ta*-C films, when nitrogen concentration increases.[6,7]

In addition to the difficulties encountered with bonding characterization, two other problems, experimentally identified, make this system attractive: one has to do with the existence of a real upper limit found for the concentration of nitrogen in a carbon matrix; the other is related to the behavior of nitrogen as a possible dopant at low concentrations. It is well known that it is impossible to generate amorphous CN systems with concentrations above 20%–30% nitrogen since this element simply escapes from the material at atmospheric pressure.[9,10] Also, it has been experimentally found that at concentrations less than 5%, nitrogen increases the conductivity of amorphous carbon in a manner similar to the conventional n-type doping of silicon; that is, nitrogen becomes a donor.[6,11]

Ab initio studies of this system are scarce. In recent work by Merchant *et al.* random networks were generated by melting a crystalline 64-atom supercell and quenching it afterwards.[12] They used Wannier function techniques contained in the Car Parrinello molecular dynamics (CPMD) code to describe the types of bonding, and they also studied the electronic density of states to investigate the doping mechanism of carbon by nitrogen. Only three different densities were considered, each for two concentrations, influenced by the experimental work of Walters *et al.*[13] The two concentrations were $C_{62}N_2$ and $C_{56}N_8$, and the three densities were 2.45 g/cm^3, 2.95 g/cm^3, and 3.20 g/cm^3. An additional simulation was carried out for a density of 2.7 g/cm^3 and a concentration of $C_{60}N_4$. Because of the small number of atoms in the supercell (64) and the few concentrations considered, it is difficult to see tendencies and the systematics of their results.

In previous studies by this group[14] they found that when nitrogen was substituted for an sp^2-bonded carbon atom, the site remained as threefold coordinated, and a lone-pair orbital developed. When nitrogen was substituted for an sp^3-bonded carbon atom, a bond was broken and the coordination of the site was reduced to 3. The fourth bond was lengthened to accommodate the lone-pair orbital on the nitrogen atom. They claimed that, contrary to the substitutional doping experimentally found, their results did not indicate

the presence of tetrahedral nitrogen. Due to the low concentrations of N used in both papers, the detection of some signal concerning the limit of doping with nitrogen would have been difficult.

An *ab initio* based tight binding molecular dynamics method has been used by Frauenheim and co-workers to generate amorphous CN compounds with different stoichiometries and densities.[15,16] For high density systems (≈ 3 g/cm^3) the results suggest that nitrogen catalyzes the undercoordination of carbon, which in turn causes N to develop CN double and triple bonding. The networks with low densities, around 1.5–2 g/cm^3, and high nitrogen incorporation, show a large number of terminating groups like C═N, and even the production of N_2 dimers (molecules). They argue that these N_2 molecules, under real deposition processes, will probably evaporate into the gas phase, reducing the maximum nitrogen content attainable.

In this work we report the *ab initio* generation of amorphous networks for the carbon nitrogen system up to concentrations of nearly 45% nitrogen. We start with crystalline supercells with 216 atoms of carbon and nitrogen and to avoid unnecessary parameters, the densities used are the experimental values fitted to a straight line. our method is different from the one that has been reported in the literature for decades, and that Merchant *et al.* coined as the "liquid-quench" method. Since it has become clear that the liquid-quench approach leads to amorphous samples with remnants of the liquid state, like overcoordination,[17] we decided to amorphize our supercells by heating them to a value below the melting temperature (*undermelt*), based on Poate's experimental results.[18] These results show that, for semiconductors, the glass temperature is at least tens of degrees below the melt and one can encounter disordered structures at these temperatures. After this undermelting process we *quench* the samples. Just to be as descriptive as Merchant and coworkers, we shall identify the method that we developed a few years ago as the "*undermelt-quench*" approach. Our aim in what follows is to show that our results can reproduce the two experimental facts mentioned above. We also find that the variation of *n*-fold coordinated nitrogen as a function of concentration agrees with several experiments. These results are based on what could be an assumption applicable to other covalent systems, i.e., the geometrical fact that the bond length in these amorphous systems can be taken as the first minimum of the corresponding partial radial distribution functions, especially when this minimum is zero.

II. THE UNDERMELT-QUENCH METHOD

In our previous work[17] we found it useful to employ a molecular dynamics approach developed originally by Harris to rapidly obtain the structures of atomic aggregates. These aggregates are initially disrupted randomly, then heated using molecular dynamics to foster the rearrangement of their atomic constituents and finally cooled down to what would be the structure of minimum energy, at least locally. The code uses the Harris functional[19] and therefore the process is not self-consistent. The linear combination of atomic orbitals utilized makes the minimum energy atomic structures generated very close to experiment. The interatomic distances fall within 1% of the experimental ones for a large variety of small molecules.[20,21] This is the essence of FASTSTRUCTURE_SIMANN (Ref. 20) (FAST for short) the code developed by Harris which is described in more detail in Refs. 20 and 21. Rather than using this code to find the minimum-energy atomic structure of a cell, we use it to generate random structures from an originally crystalline supercell with periodic boundary conditions. We have successfully used this code, within the undermelt-quench approach, to generate random atomic networks of silicon, hydrogenated silicon, silicon-nitrogen alloys, carbon, germanium, porous silicon, porous carbon, aluminum, and aluminum-nitrogen alloys.[17]

The undermelt-quench method is not designed to reproduce the way an amorphous material is grown, but has the objective of generating amorphous samples that represent adequately those obtained experimentally. In this work we amorphize crystalline, diamondlike structures with 216 atoms in the cell [$(216-y)$ carbons, y randomly substituted nitrogens and a concentration $c=(y/216)\times 100$, by linearly heating each sample, using FAST, from 300 K to a value below the melting temperature, in 100 steps of 4 fs and immediately cooling them down to 0 K in 108 steps. A process like this has been applied to carbon[22] where a high temperature of 3700 K was used obtaining radial distribution functions (RDFs) very close to experimental. In this manner we avoid melting the system and then quenching it from the molten state. Due to the lack of information concerning the melting temperatures of the CN system we decided to use the value of 3700 K for all samples (see also Ref. 22), which is below the melting temperature of pure carbon. Since the time step and the melting temperature were kept constant, the heating/cooling rate was 8.50×10^{15} K/s. The atoms were allowed to move within each cell with periodic boundary conditions, whose volume was determined by the corresponding experimental density and concentration. We next subjected them to annealing cycles at 300 K, with intermediate quenching steps down to 0 K. At the end of the process a geometry optimization was carried out to find the amorphous structures with a local energy minimum. The densities considered were obtained from experimental data although the experimental dispersion is noticeable and depends strongly on the deposition procedure utilized to generate the samples.[5] In our work a linear fit is adjusted to the experimental data: $\rho=2.897-1.784c$, where c is the nitrogen concentration; the density values for each of the 9 nitrogenated samples, plus the pure carbon sample, are listed in Table I.

One would think that the undermelt-quench approach may be dependent on the initial crystalline structures used, but we have demonstrated that starting with diamondlike low-density carbon structures we generated RDFs that are indistinguishable from those obtained from initial hexagonal or rhombohedral structures.[23]

FAST uses optimization techniques through a force generator to allow simulated annealing/molecular-dynamics studies with quantum force calculations.[24] For our study we use the local density approximation (LDA) due to Vosko, Wilk, and Nusair (VWN),[25] since it has been reported that the number of unpaired spins in amorphous carbon-nitride is low;[26] this is the density approximation that we have used in our previous work.

TABLE I. Concentrations and densities for a-CN_x.

Sample	N concentration (%)	Density (g/cm^3)
$C_{216}N_{00}$	0.0	2.90
$C_{205}N_{11}$	5.1	2.81
$C_{194}N_{22}$	10.2	2.72
$C_{184}N_{32}$	14.8	2.63
$C_{173}N_{43}$	19.9	2.54
$C_{162}N_{54}$	25.0	2.45
$C_{151}N_{65}$	30.1	2.36
$C_{140}N_{76}$	35.2	2.27
$C_{130}N_{86}$	39.8	2.19
$C_{119}N_{97}$	44.9	2.10

Carbon and nitrogen have such a low number of electrons that an all electron calculation can be carried out. We used a minimal basis set, consisting of the atomic orbitals occupied in the neutral atom, with a cutoff radius of 3.5 Å for the amorphization and for the optimization. For each atom, one function is used to represent the core part of the electron density and one to represent the valence part of the electron density. The physical masses of carbon and nitrogen are always used and this allows the visualization of realistic randomizing processes of all the atoms during the amorphization of the supercell. In order to better simulate the dynamical processes that occur during the amorphization in reasonable computer time, a time step of 4 fs was used throughout.[22] The forces are calculated using rigorous formal derivatives of the expression for the energy in the Harris functional, as discussed by Lin and Harris.[24] The evaluation of the 3-center integrals that contribute to the matrix elements in the one-particle Schrödinger equation is the time-limiting feature of FAST and each is performed using the weight-function method of Delley.[27]

III. RESULTS AND DISCUSSION

A difficult problem in amorphous materials is finding a criterion to determine when two atoms are still considered bonded. Some authors have carried out extensive searches for possible molecular (cluster) structures of a given element, silicon for example, to infer a possible bond length.[28] Others opted for the use of localized wave functions, like the Wannier-type, to get an estimate of the bond lengths.[12] One can also look at the charge distribution between atoms and set a limit below which the bonding is declared nonexistent. We decided to use a geometrical approach to the problem. We believe that the structure of radial distribution functions is a manifest way to determine the *maximum* bond length, especially when there is a clear zero minimum between the first and the second peaks, which is the case for most elemental amorphous semiconductors. When amorphous alloys are considered, a way to determine the bond lengths among the diverse species is by looking at the minimum between the first and second peaks of the corresponding *partial* RDFs (pRDFs); the maximum bond length is then set equal to the position of these minima. Using this approach we can determine the extension of the bond, and also the number of neighbors by integrating the area under the corresponding peak; it is difficult to determine the multiplicity of the bonds (single, double or triple) using this method. In what follows we use this approach since the first minima of the corresponding pRDFs are the same for all concentrations and are given by 2.0 Å for C-C, 1.9 Å for C-N, and 1.8 Å for N-N.[29]

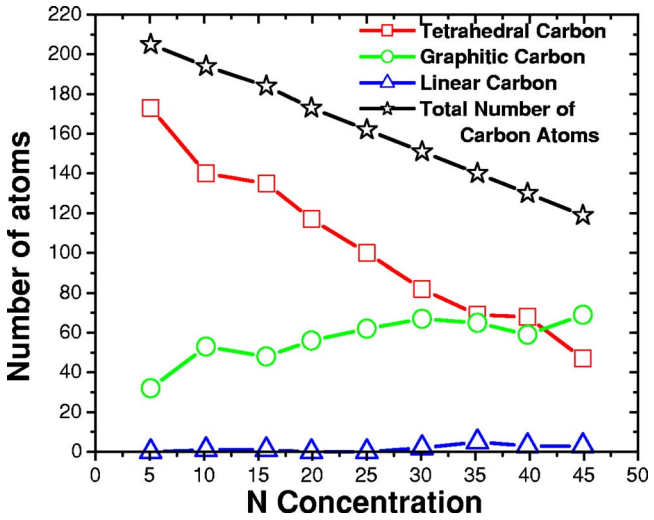

FIG. 1. (Color online) The bonding nature of carbon as a function of nitrogen concentration. The tetrahedral carbon (squares) decreases whereas the graphitic carbon (circles) increases as the nitrogen concentration increases.

Based on this assumption we proceeded to obtain the number of nearest neighbors to any carbon or any nitrogen as a function of nitrogen concentration. In this paper we focus mainly on the nearest neighbors to nitrogens, in order to investigate the two experimental results mentioned above; namely, the fact that nitrogen becomes tetrahedrally coordinated at low concentrations and the fact that there is an experimental upper limit to the nitrogen concentration in an amorphous carbon matrix. Once the maxima of the bond lengths are set, then the number of nitrogen atoms that are singlefold, twofold, threefold, and fourfold (overcoordinated) coordinated can be determined; no fivefold or higher bonding arrangements were found.

In Fig. 1 the dependence of the bonding nature of carbon with nitrogen concentration is presented. Evidently, the total number of carbon atoms diminishes linearly as the number of nitrogens increase, and there is an almost linear variation of tetrahedral and graphitic carbon. Tetrahedral (fourfold) carbons show a plateau between 10% and 15% and another between 35% and 40%; linear (twofold) carbons begin appearing at 30% and graphitic (threefold coordinated) carbons behave in a complementary manner. No fivefold coordinated carbons were found. At about 15% nitrogen, graphitic carbons diminish and, correspondingly, tetrahedral carbons increase; at 35% the number of graphitic and tetrahedral carbons is practically the same, whereas linear carbons acquire a nonzero value. For concentrations larger than 40% graphitic

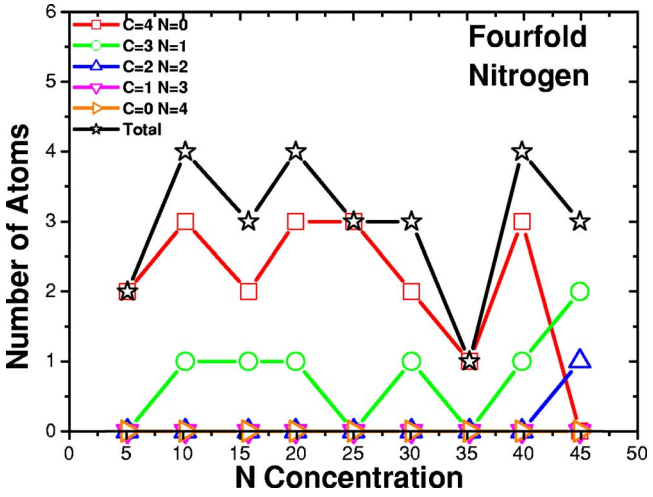

FIG. 2. (Color online) Tetrahedral (dopant) nitrogens are prominent at low concentrations, 0–10%. This behavior is masked by other types of bonding for higher concentrations. Bonding to 4 carbons is represented by squares; to 3 carbons and one nitrogen by circles.

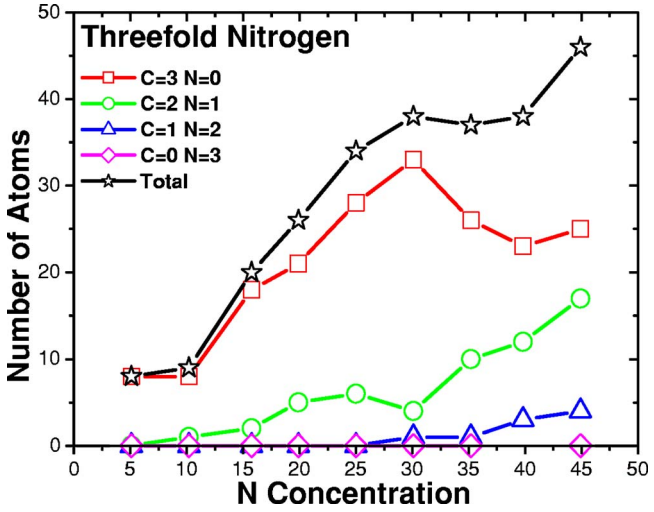

FIG. 3. (Color online) Nitrogens triple bonded. The total number is practically constant between 5% and 10%. The squares are nitrogens bonded to three carbons; the circles are nitrogens bonded to two carbons and one nitrogen.

carbons outnumber tetrahedral carbons and linear carbons are distinctively finite. This behavior indicates a slight departure from linearity at about 10% and 35%; this departure could be related to the behavior of nitrogen as a dopant below 10% and to the saturation limit around 35%; clearly more information is needed to support this point.

In order to further investigate the bonding structure of these alloys we looked at the possibility of finding fourfold (overcoordinated) nitrogens for certain concentrations. In fact, at 5% (the lowest concentration of nitrogen we investigated) the first sign of overcoordination appears and this is due to the coordination of one nitrogen with four carbons, Fig. 2. Such overcoordination should manifest itself at concentrations lower than 5% if continuity in the behavior is to be expected. This fourfold coordination leads to the appearance of an electronic state within the energy gap.[30] It is interesting to note that fourfold coordination due to three carbons and one nitrogen is also important in this region. As the number of nitrogen atoms increases the preponderance of these fourfold coordinated atoms becomes less relevant since they remain constant whereas other types of bonding become more prominent. See total curves in Figs. 3 and 4.

Figure 3 shows how threefold coordination of nitrogen with three carbons appears at 5% and increases up to 30%. Thereafter it decreases while an important rise of the coordination with two carbons and one nitrogen begins. Coordination with one carbon and two nitrogens starts growing at 25%, whereas threefold coordination with three nitrogens never appears in the range studied. It is clear that something drastic happens at 30% since the threefold coordination with three carbons starts diminishing abruptly. We believe this is another indication of the existence of an upper limit to the nitrogen incorporation into an amorphous carbon matrix.

Double bonded nitrogen appears at larger concentrations (10%) and continously increases up to 45%, Fig. 4. A plateau is observed between 10% and 15% for the total twofold coordination and for nitrogen bonded to two carbons. Double bonded nitrogen to one carbon and one nitrogen increase slowly but is always smaller than the previous case. Finally, twofold coordination to two nitrogens is nonexistent except at the highest concentration.

Figure 5 shows that single bonded (singlefold) nitrogen coordinated to one carbon exists starting at 25%; it has a maximum at about 35%–40% and then begins to decrease [red (dark gray) squares]. Something similar occurs with the appearance of N-N coordination [green (light gray) circles] since it begins at 30%, two singlefold nitrogen atoms appear at 35%, reaches a maximum of four at 40%, and then diminishes. This behavior indicates the potential formation of nitrogen molecules N_2 in the system. But why should we have molecular nitrogen in our amorphous alloys for large concen-

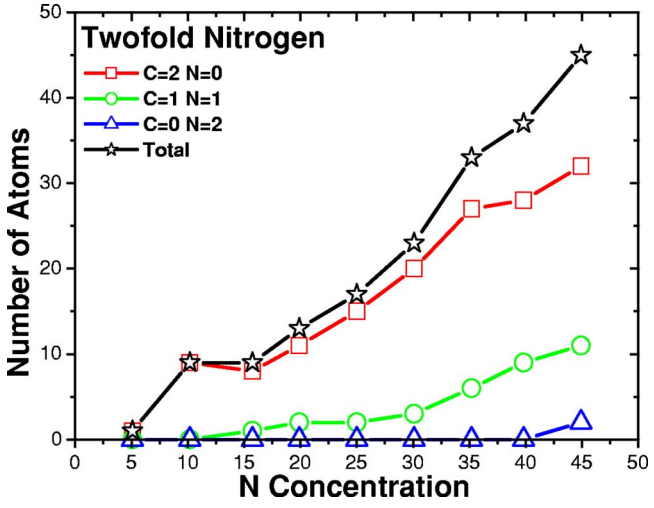

FIG. 4. (Color online) Nitrogen double bonded. The total number is practically zero at 5%, shows a plateau between 10% and 15% and increases systematically afterwards. Squares represent carbons bonded to two nitrogens and circles to one carbon and one nitrogen.

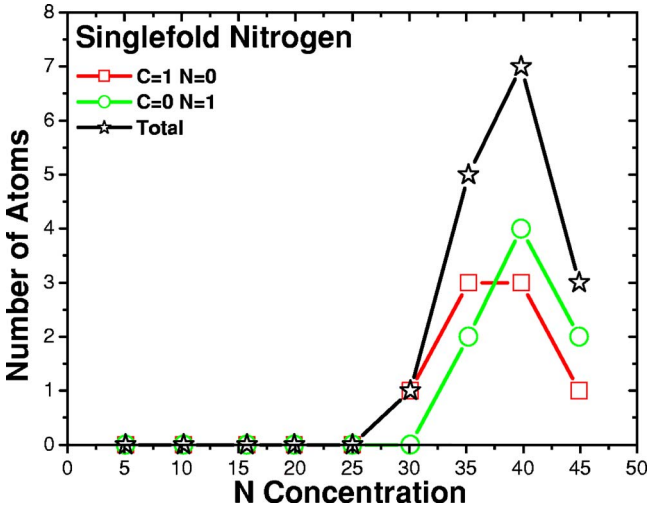

FIG. 5. (Color online) Single bonded nitrogens appear only at concentrations larger than 25%. There are nitrogens bonded to one carbon (squares) and to another nitrogen, molecular nitrogen (circles).

trations? The explanation is the following. Since our approach does not allow nitrogens to abandon the cubic supercell when a saturation concentration is reached, the nitrogen cannot leave the material and therefore remains in the gaseous state within the CN system; eventually it forms molecules that appear in the voids of the supercell. This explanation is explicitly corroborated in Figs. 6–8, where the molecules are shown: one for 35% (1.26 Å interatomic distance), two for 40% (1.25 Å and 1.26 Å), and one for 45% (1.25 Å). It is clear then that this phenomenon signals the presence of a saturation limit in the CN system.

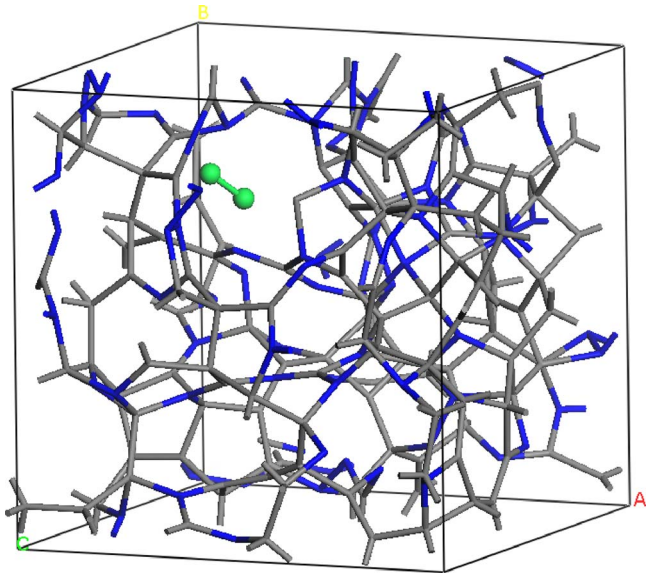

FIG. 6. (Color online) For concentrations above 25% single bonded nitrogen exists. At 35% a nitrogen molecule [green (light gray) dumbbell] appears signaling the saturation limit to nitrogen incorporation. Carbon: light gray sticks; nitrogen: blue (black) sticks.

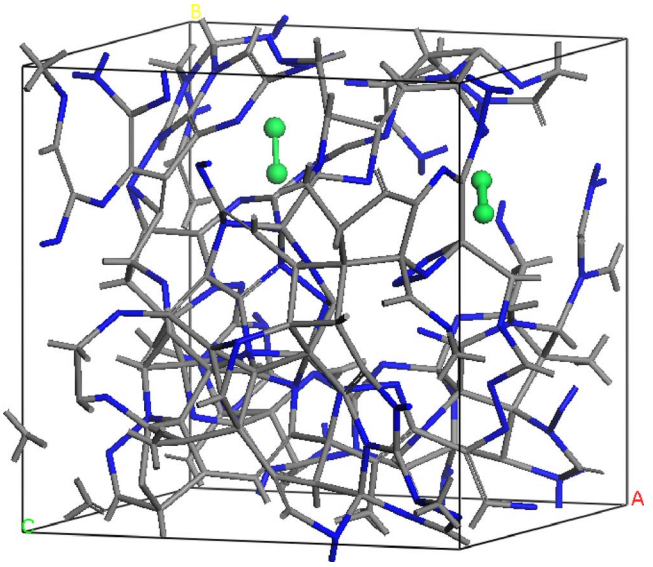

FIG. 7. (Color online) At a concentration of 39.8% two nitrogen molecules [green (light gray) dumbbells] appear indicating that we are already within the saturation region. Carbon: light gray sticks; nitrogen: blue (black) sticks.

IV. ANALYSIS AND CONCLUSIONS

Carbon bonding is versatile; conventionally, three different types of hybridizations are attributed to carbon, fourfold sp^3, threefold sp^2, and twofold sp^1 with precise orientations. In amorphous materials with carbon content it is difficult to talk about the orientation of bonds since the resulting structure is not geometrically well defined; nevertheless these three hybridizations are invoked as a basis of analysis of the atomic topology. Nitrogen bonding is also versatile since nitrogen has five valence electrons and it also manifests three different types of hybridizations. However, the electronic ar-

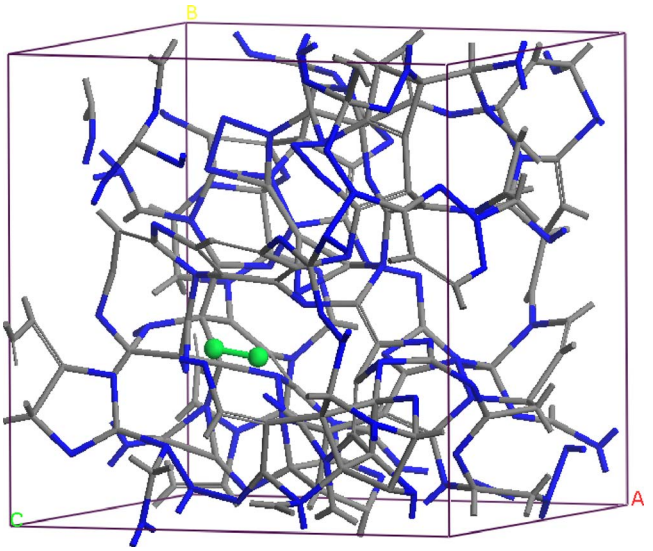

FIG. 8. (Color online) At a 44.9% concentration of nitrogen N_2 molecules still exist [green (light gray) dumbbell], well within the saturation region. Light gray sticks correspond to carbon, blue (black) sticks correspond to nitrogens.

rangement is somewhat different since electron lone pairs appear. A thorough analysis of the possible bonds in the crystalline or molecular CN system leads to nine different structures.[4] If we now realize that the arrangements in an amorphous system are not at all well organized one can see that the amorphous CN system is very complex and that its bonding structures are difficult to characterize.

In the present work we have applied our undermelt-quench *ab initio* process to generate amorphous networks of $C_{1-x}N_x$ alloys ($0 \leqslant x \leqslant 0.45$). To compare our results to experiment we decided to use a fitting to the experimental densities found in the literature, although this leaves out interesting studies of the bonding behavior of high density (sp^3 bonded) and low density (sp^2 bonded) samples for a given concentration of nitrogen. We also opted for the geometric approach to determine the bond length and looked at the first minima of the partial RDFs as a criterion for the maximum extension of the bonds among the elements. This cutoff allowed us to unambiguously talk about nearest neighbors for a given atom. Based on this approach we conclude that:

(i) Tetrahedral nitrogen (*ta*-N) appears in our *ab initio* generated CN samples. The amount of *ta*-N is essentially constant and small (Fig. 2), for all concentrations studied and therefore becomes more relevant for concentrations below 5% where the number of other *n*-fold coordinated nitrogens, with $n \leqslant 3$, is also small. At higher concentrations *ta*-N exists but its presence is masked by all the other bonding arrangements of nitrogen (Figs. 3–5). These results are in agreement with the EELS experiments reported in the literature.

(ii) For concentrations higher that 30% singlefold nitrogen appears bonded to another nitrogen, giving rise to N_2 molecules (Figs. 6–8). We take this as signaling the onset of an upper limit for the incorporation of N in an amorphous carbon matrix, in agreement with experiment and supporting the surmise that the saturation of the nitrogen content within the films is due to the formation of molecular nitrogen either at or below the film surface.[9] Another indication that something drastic happens at 30% is that the threefold coordination of nitrogen with three carbons starts diminishing abruptly, Fig. 3.

Our results also show the essentially linear decrease of the sp^3 carbon fraction with increasing nitrogen concentration reported experimentally, and the corresponding increase of the sp^2 carbon fraction, Fig. 1. This behavior suggests that for the densities used, carbon atoms bonded to nitrogen revert to sp^2 bonding. It is then clear that unlike what happens in the SiN system, where nitrogens immediately surround themselves with practically 3 Si, saturating their valence,[31] in CN the situation is more varied.

The agreement of our findings with experimental results indicates that our undermelt-quench method generates random networks which adequately describe the experimental tendencies in amorphous covalent material systems. Therefore, using the generated structures it is possible to characterize the atomic topology of the systems and knowing the atomic topology, the electronic and optical properties of these materials can be calculated. We hope our results may stimulate further experimental and theoretical studies in the area.

ACKNOWLEDGMENTS

A.A.V. thanks DGAPA-UNAM for financing Projects Nos. IN101798, IN100500, and IN119105. This work was performed on an Origin 2000 computer provided by DGSCA, UNAM. M. T. Vazquez and S. Jimenez provided the information requested.

*Electronic address: valladar@servidor.unam.mx

[1] D. R. McKenzie, Rep. Prog. Phys. **59**, 1611 (1996).
[2] J. Robertson, Prog. Solid State Chem. **21**, 199 (1991); J. Robertson, Mater. Sci. Eng., R. **37**, 129 (2002).
[3] E. Kroke and M. Schwarz, Coord. Chem. Rev. **248**, 493 (2004).
[4] S. P. R. Silva, J. Robertson, G. A. J. Amaratunga, B. Rafferty, L. M. Brown, J. Schwan, D. F. Franceschini, and G. Mariotto, J. Appl. Phys. **81**, 2626 (1997).
[5] Sandra E. Rodil, Ph.D thesis, University of Cambridge, U K, November 2000.
[6] C. A. Davis, D. R. McKenzie, Y. Yin, E. Kravtchinskaia, G. J. A. Amaratunga, and V. S. Veerasamy, Philos. Mag. B **69**, 1133 (1994).
[7] X. Shi, H. Fu, J. R. Shi, L. K. Cheah, B. K. Tay, and P. Hui, J. Phys. C **10**, 9293 (1998); A. Stanishevsky, L. Khriachtchev, and I. Akula, Diamond Relat. Mater. **7**, 1190 (1998); M. Chhowalla, I. Alexandrou, C. Kiely, G. A. J. Amaratunga, R. Aharonov, and R. Fontana, Thin Solid Films **290-291**, 103 (1996).
[8] K. S. Yoo, B. Miller, R. Kalish, and X. Shi, Electrochem. Solid-State Lett. **2**, 233 (1999).
[9] D. Marton, K. J. Boyd, A. H. Al-Bayati, S. S. Todorov, and J. W. Rabalais, Phys. Rev. Lett. **73**, 118 (1994); D. Marton, K. J. Boyd, and S. W. Rabalais, Mod. Phys. Lett. B **9**, 3527 (1995).
[10] F. D. A. Aarao Reis and D. F. Franceschini, Appl. Phys. Lett. **74**, 209 (1999).
[11] V. S. Veerasamy, G. A. J. Amaratunga, C. A. Davis, A. E. Timbs, W. I. Milne, and D. R. McKenzie, J. Phys.: Condens. Matter **5**, L169 (1993).
[12] A. R. Merchant, D. R. McKenzie, and D. G. McCulloch, Phys. Rev. B **65**, 024208 (2001).
[13] J. K. Walters, M. Kuhn, C. Spaeth, H. Fischer, F. Richter, and R. J. Newport, Phys. Rev. B **56**, 14315 (1997).
[14] D. R. McKenzie, E. G. Gerstner, A. R. Merchant, D. G. McCulloch, P. E. Goa, N. C. Cooper, and C. M. Goringe, Int. J. Mod. Phys. B **14**, 230 (2000).
[15] F. Weich, J. Widany, and Th. Frauenheim, Phys. Rev. Lett. **78**, 3326 (1997).
[16] Th. Frauenheim, G. Jungnickel, P. Sitch, M. Kaukonen, F. Weich, J. Widany, and D. Porezag, Diamond Relat. Mater. **7**, 348 (1998).
[17] A. A. Valladares, F. Alvarez, Z. Liu, J. Stitch, and J. Harris, Eur. Phys. J. B **22**, 443 (2001); F. Alvarez and A. A. Valladares, Appl. Phys. Lett. **80**, 58 (2002); F. Alvarez, C. C. Díaz, A. A. Valladares, and R. M. Valladares, Phys. Rev. B **65**, 113108-1

(2002); F. Alvarez and A. A. Valladares, J. Non-Cryst. Solids **299-302**, 259 (2002); Rev. Mex. Fis. **48**, 528 (2002); Solid State Commun. **127**, 483 (2003); E. R. L. Loustau, R. M. Valladares, and A. A. Valladares, J. Non-Cryst. Solids **338-340**, 416–420 (2004); E. Y. Peña, M. Mejía, J. A. Reyes, R. M. Valladares, F. Alvarez, and A. A. Valladares, *ibid.* **338-340**, 258 (2004); Ariel A. Valladares, J. Non-Cryst. Solids (unpublished).

[18] J. M. Poate, in *Electronic Materials. A New Era in Materials Science*, edited by J. R. Chelikowsky and A. Franciosi (Springer-Verlag, Berlin, Heidelberg, 1991), p. 323.

[19] J. Harris, Phys. Rev. B **31**, 1770 (1985).

[20] FastStructure_SimAnn, User Guide, Release 4.0.0 (San Diego, Molecular Simulations, Inc., September 1996).

[21] Xiao-Ping Li, J. Andzelm, J. Harris, and A. M. Chaka, in *Chemical Applications of Density-Functional Theory*, edited by B. B. Laird, R. B. Ross, and T. Ziegler (American Chemical Society, Washington, D.C., 1996), Chap. 26.

[22] F. Alvarez, C. C. Díaz, R. M. Valladares, and A. A. Valladares, Diamond Relat. Mater. **11**, 1015 (2002).

[23] C. Romero, Z. Mata, M. Lozano, H. Barrón, R. M. Valladares, F. Alvarez, and Ariel A. Valladares, J. Non-Cryst. Solids **338-340**, 513 (2004).

[24] Z. Lin and J. Harris, J. Phys.: Condens. Matter **5**, 1055 (1992).

[25] S. H. Vosko, L. Wilk, and M. Nusair, Can. J. Phys. **58**, 1200 (1980).

[26] F. Demichelis, X. F. Xong, S. Schreite, A. Tagliaferro, and C. E. Martino, Diamond Relat. Mater. **4**, 361 (1995); see also Ref. 12.

[27] B. Delley, J. Chem. Phys. **92**, 508 (1990).

[28] S. Kugler and Z. Varallyay, Philos. Mag. Lett. **81**, 569 (2001). S. Kugler, K. Kohary, K. Kadas, and L. Pusztai, Solid State Commun. **127**, 305 (2003).

[29] A. A. Valladares and F. Álvarez-Ramírez (unpublished).

[30] Ariel A. Valladares, Alexander Valladares, Renela M. Valladares, and Mary A. McNelis, J. Non-Cryst. Solids **231**, 209 (1998).

[31] F. Alvarez and A. A. Valladares, Phys. Rev. B **68**, 205203-1 (2003).